DARK ENERGY: AN OBSERVATIONAL PRIMER*

Ramon Miquel

Institució Catalana de Recerca i Estudis Avançats
Institut de Física d'Altes Energies
Edifici Cn, Campus UAB, 08193 Bellaterra (Barcelona), Spain

(Received August 18, 2008)

After a short introduction to the equations of FLRW Cosmology, I review the four main techniques used to understand observationally the properties of dark energy in turn, followed by a short summary of the current understanding of the subject. I finalize with a description of a few of the main dark-energy oriented surveys that are going to take place in the near future.

PACS numbers: 95.36.+x, 98.80.–k, 98.80.Cq

1. Introduction

In 1998, the study of the redshift-luminosity relation (Hubble diagram) for near-by and distant supernovae [1, 2] provided the "smoking gun" for the accelerated expansion of the universe and the existence of the mechanism that drives it, code-named "dark energy". Since then, more supernova plus Cosmic Microwave Background (CMB) and Large Scale Structure (LSS) measurements have confirmed that we live in an accelerating universe. All observations can be explained within a flat Friedmann–Lemaître–Robertson–Walker (FLRW) universe which is made of about 75% dark energy, about 20% dark matter and less than 5% ordinary matter. While candidates for dark matter abound, the nature of dark energy is much more mysterious. It could be Einstein's cosmological constant, a new dynamical field ("quintessence"), or nothing at all, and we would have to modify the equations of General Relativity ("modified gravity").

The US Dark Energy Task Force (DETF) report published in 2006 [3] highlighted four techniques (galaxy clustering and, in particular, baryonic acoustic oscillations (BAO); galaxy cluster counts; type-Ia supernovae as distance indicators; and weak gravitational lensing) that show the most promise

* Presented at the XXXVI International Meeting on Fundamental Physics, Baeza (Jaén), Spain, February 4–8, 2008.

in unveiling the mystery of the nature of the dark energy component of the universe that drives its current accelerated expansion. Each technique has its own strengths and weaknesses. Combining them it is possible to both gain statistical sensitivity by breaking parameter degeneracies of individual probes and be more robust to systematic effects.

Two of the techniques (supernovae and BAO) are purely geometrical, while the other two (weak lensing and clusters) probe both the geometry of the universe and its dynamics through structure growth. By combining probes of the two kinds one hopes to disentangle the effects of modified gravity from those of true dark energy.

The outline of this note is as follows. In Section 2 we briefly recall the equations of FLRW cosmology, while we discuss the four techniques in turn in Section 3. The current status of knowledge of dark energy is given in Section 4. Some of the proposed future surveys are reviewed in Section 5.

2. Cosmology

Assuming that the universe is homogeneous and isotropic at large scales leads to the Friedman–Lemaître–Robertson–Walker (FLRW) universe defined by the metric $ds^2 = dt^2 - a^2(t)(dr^2/(1-kr^2) + r^2(d\theta^2 + \sin^2\theta d\phi^2))$, where t is the proper time and (r, θ, ϕ) are co-moving coordinates. For a flat universe, that we will assume in most of the following, $k = 0$. For the FLRW metric, Einstein's field equations of general relativity reduce to the so-called Friedman–Lemaître equations:

$$\frac{\ddot{a}}{a} = -\frac{4\pi G}{3}(\rho + 3p)\,, \tag{2.1}$$

$$\left(\frac{\dot{a}}{a}\right)^2 = \frac{8\pi G}{3}\rho - \frac{k}{a^2}\,. \tag{2.2}$$

From the first equation, it is clear that in order for the expansion of the universe to accelerate ($\ddot{a} > 0$), it is necessary that $\rho + 3p < 0$, or $w < -1/3$.

Since both ρ and p evolve with time, in order to solve for $a(t)$ we need an extra equation. This can be the equation of state for each component of the universe, relating its energy density with its pressure. For matter (ordinary or dark), $p = 0$, so $w = 0$. For radiation, we have the relativistic gas relationship $p = \rho/3$, so $w = 1/3$. For the cosmological constant one has $p = -\rho$, or $w = -1$. Assuming a flat universe, Eqs. (2.1), (2.2) can be used to obtain the relationship

$$\frac{d\rho}{da} = -3(1+w)\frac{\rho}{a}\,, \tag{2.3}$$

from which, assuming a constant equation of state w, one gets:

$$\rho = \rho_0 a^{-3(1+w)}\,, \tag{2.4}$$

which results in $\rho = \rho_0 a^{-3} = \rho_0(1+z)^3$ for matter, $\rho = \rho_0 a^{-4} = \rho_0(1+z)^4$ for radiation, and $\rho = \rho_0$ for a cosmological constant. Introducing the Hubble parameter $H = \dot{a}/a$ and defining the critical density as $\rho_{\rm c} = 3H_0/8\pi G$, where H_0 is the Hubble parameter now, we can cast Eq. (2.2) as

$$H^2 = H_0^2 \left[\Omega_{\rm M}(1+z)^3 + \Omega_{\rm r}(1+z)^4 + \Omega_{\rm DE}(1+z)^{3(1+w_{\rm DE})}\right]\,, \tag{2.5}$$

where we have introduced the current normalized densities $\Omega_i \equiv \rho_0^i/\rho_{\rm c}$, for $i =$ M (matter), r (radiation) and DE (dark energy). The term proportional to $\Omega_{\rm r}$ can be safely neglected for all purposes, at least for moderate values of z ($z < 5000$). It is clear from this equation that by measuring H at different times (the history of the expansion of the universe as provided by type-Ia SNe), one can learn about the properties of the constituents of the universe, $\Omega_{\rm M}, \Omega_{\rm DE}, w_{\rm DE}$, *etc.*

3. Four techniques

3.1. Supernovae

Observationally, type-Ia supernovae are defined as supernovae without any hydrogen lines in their spectrum, but with a prominent, broad silicon absorption line (Si-II) at about 600 nm in the supernova rest frame. The progenitor is understood to be a binary system in which a white dwarf (no hydrogen) accrets material from a companion star (possibly another white dwarf). The process continues until the mass of the white dwarf approaches the Chandrasekhar limit, at which point a thermonuclear runaway explosion is triggered.

The fact that all type-Ia SNe have a similar mass[1] helps explain their remarkably homogeneity. Type-Ia SNe are very homogeneous in luminosity, color, spectrum at maximum light, *etc.* Only small and correlated variations of these quantities are observed. They are very bright events with absolute magnitude in the B-band reaching $M_B \sim -19.5$ at maximum light. The raise time and decay time of their light curve (magnitude as a function of time) are, respectively, 15–20 days and ~ 2 months, in the SN rest frame.

In 1992 Mark Phillips [5] found that for near-by SNe there was a clear correlation between their intrinsic brightness at maximum light and the duration of their light curve, so that brighter SNe last longer (see Fig. 1).

[1] See [4] for an intriguing exception.

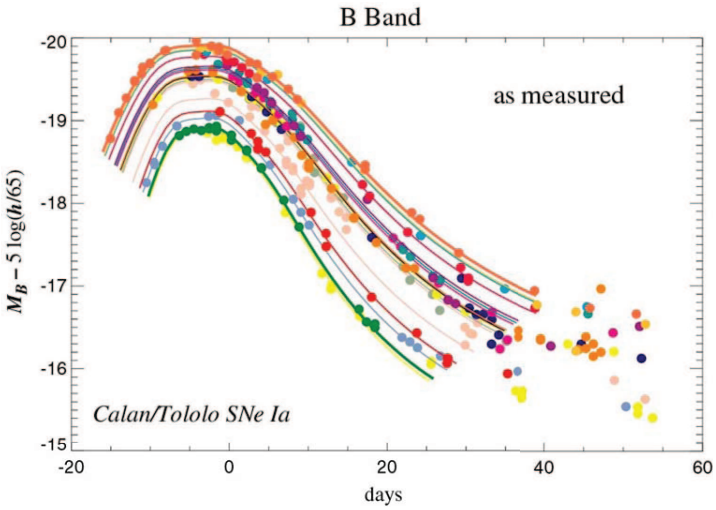

Fig. 1. *B*-band light curves of the Calán/Tololo type-Ia supernova sample before any duration-magnitude correction.

Several empirical techniques [6–9] have been developed since then to make use to this correlation to turn type-Ia SNe into standard candles, with a dispersion on their peak magnitude of only 0.10–0.15 mag, corresponding to a precision of about 5–7% in distance, and, therefore, in lookback time to the explosion. Fig. 2 shows the same SNe light curves of Fig. 1 after applying the "stretch" technique of [6], so called because it basically amounts to a simple stretching of the time axis, showing the good uniformity achieved.

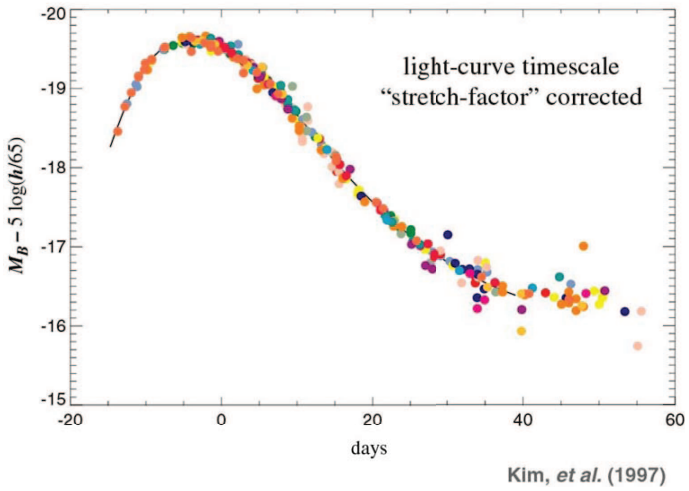

Fig. 2. Same light curves of Fig. 1 after applying the "stretch" duration-magnitude correction of Ref. [6].

While light-curves are determined with photometric measurements in several broadband filters, spectroscopy near maximum light serves the dual purpose of unambiguously identifying the object as a type-Ia SN and at the same time determining its redshift. Both goals are achieved by comparing the measured spectrum to templated spectra from well-measured near-by type-Ia supernovae. The key feature of the spectrum is the Si-II absorption line, whose detection identifies the SN as a type Ia, and whose position determines the redshift. Fig. 3 shows spectra of three supernovae: from top to bottom, a type II, a type Ia, and a type Ic . The Si-II feature can be seen clearly in the type-Ia spectrum.

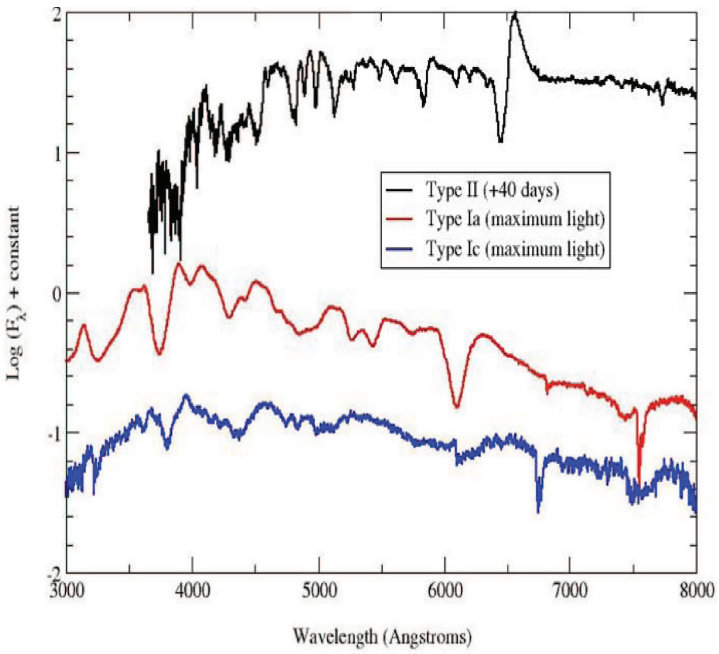

Fig. 3. Measured spectra of three supernovae. From top to bottom: type II, type Ia, type Ic. The Si-II feature identifying a type-Ia SNe is clearly visible in the middle spectrum at about 600 nm.

3.1.1. The Hubble diagram

Once the stretch-corrected magnitude and redshift are determined, the supernova can be put into a Hubble diagram in order to measure the cosmological parameters. The Hubble diagram is a plot of measured magnitude *versus* redshift. Since the apparent magnitude of a standard candle gives us its distance and the time t at which the light was emitted, and the red-

shift gives the cosmic expansion parameter $a(t)$, a Hubble diagram populated with SNe at different distances gives us the history of the expansion of the universe. Since the expansion rate of the universe is determined by its matter-energy content, it is clear that type-Ia SNe can tell us about the properties of the contents of the universe, and, in particular, of the dark energy component.

Standard candles (or, in the case of type-Ia SNe, "standardizable" candles) provide a measurement of the luminosity distance $d_{\rm L}$ as a function of redshift. $d_{\rm L}$ can be defined through the relation $\phi = \frac{L}{4\pi d_{\rm L}^2}$, where L is the intrinsic luminosity, and ϕ the flux, so that $d_{\rm L}$ is the "equivalent distance" in a Euclidean, non-expanding universe. It is easy to see that $d_{\rm L}(z) = (1+z)\, r(z)$, where $r(z)$ is the co-moving distance to the source at redshift z. Recalling that light travels in geodesics ($ds^2 = 0$), we can easily compute $r(z)$ from the FLRW metric as

$$r(z) = \int_1^2 dr = \int_1^2 \frac{dt}{a} = \int_1^2 \frac{da}{a\dot{a}} = \int_0^z \frac{dz'}{H(z')}\,, \tag{3.1}$$

where for simplicity we have assumed a flat universe. Astronomers measure fluxes as apparent magnitudes:

$$\begin{aligned} m(z) &\equiv -2.5\log\left(\phi/\phi_0\right) = \mathcal{M} + 5\log\left[H_0 d_{\rm L}(z)\right]\,, \\ \mathcal{M} &\equiv M + 25 - 5\log\left[H_0/100\,{\rm kms}^{-1}{\rm Mpc}^{-1}\right]\,, \end{aligned} \tag{3.2}$$

where M is the (assumed unknown) absolute magnitude of a type-Ia SN, related to $-2.5\log L$. The flux ϕ_0 defines the zero point of the magnitude system used. It should become clear from Eqs. (3.1) and (2.5) that, contrary to the appearances, Eq. (3.2) does not depend on H_0. An example of a Hubble diagram can be seen in Fig. 4. By measuring apparent magnitudes and redshifts from a set of type-Ia supernovae, one can measure different integrals of $H_0/H(z)$, which according to Eq. (2.5) are sensitive to the cosmological parameters. Note that in the standard cosmological analyses $\mathcal{M}$ is considered a nuisance parameter and it is determined simultaneously from the data.

The goal of the near-future type-Ia supernova surveys is to help determine the properties of the dark energy component of the universe, as encoded in its equation of state parameter $w \equiv p/\rho$, where p is its pressure and ρ its energy density. The equation of state parameter is customarily parametrized as [10, 11] $w(z) = w_0 + w_a\,(1-a)$, where w_0 is the equation of state parameter now (which has to fulfill $w_0 < -1/3$ in order to drive the current accelerated expansion of the universe), and $w_a = -dw/d\ln a|_0$

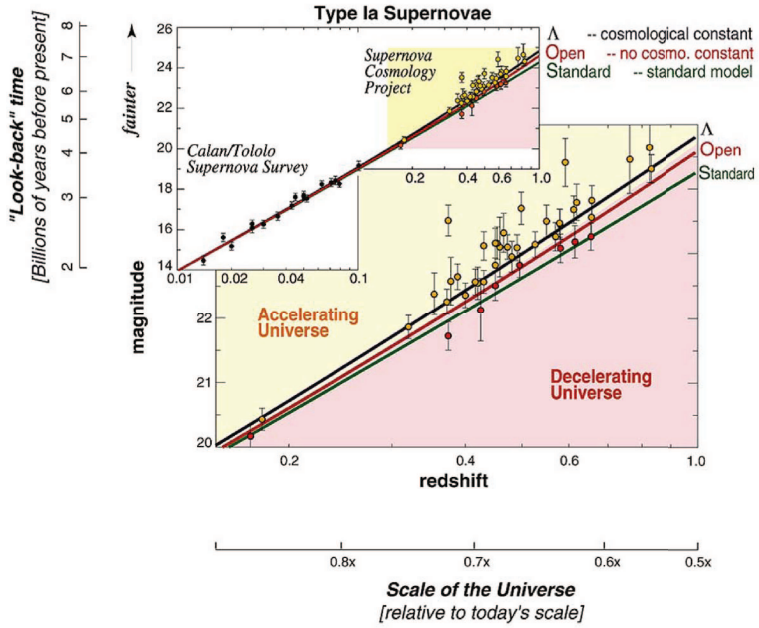

Fig. 4. Example of apparent magnitude *versus* redshift Hubble diagram, from the 1998 Supernova Cosmology Project results [1].

is a measure of the current rate of change of w with time. Here z is the redshift and $a = (1+z)^{-1}$ is the expansion parameter of the universe, with the current value being $a_0 = 1$, corresponding to $z = 0$. For a cosmological constant, we have $w_0 = -1$, $w_a = 0$. A first goal is to determine w_0 and w_a with enough accuracy to establish whether the dark energy is "just" a cosmological constant or it has a dynamical origin.

3.1.2. Systematic uncertainties

The reach in w_0 and w_a in current and future high-statistics type-Ia SNe surveys is already limited by systematic uncertainties. A lot of effort is being put in gathering well-measured (both photometrically and spectroscopically) samples of near-by SNe [12,13] in order to study their properties in detail and constrain the systematic uncertainties. In designing new surveys it is of the utmost importance to pay attention to systematics. Predictions based solely on statistical reach are doomed to be proved over-optimistic and misleading when data arrive.

The statistical uncertainties in the Hubble diagram are dominated by the intrinsic supernova peak magnitude dispersion $\sigma_{\rm int} = 0.10$–0.15. Since this error is uncorrelated from supernova to supernova, in a redshift bin

with $\mathcal{O}(100)$ SNe (a quantity most current and all near-future surveys will achieve), the statistical error will be $\sigma_{\rm stat} = 0.01$–0.02. Since many systematic uncertainties are expected to be fully correlated for SNe at similar redshifts, but uncorrelated otherwise, it is clear that systematic errors of the order of a few per cent will be important, and, in many cases, already dominant.

A comprehensive study of systematic errors affecting type-Ia SNe distance measurements can be found in [14]. We will only cover the more relevant ones in the following.

Dust in the path between the supernova and the telescope attenuates the amount of light measured. Milky Way dust is well measured and understood [15], while intergalactic dust has a negligible effect. In contrast, dust in the supernova host galaxy can lead to a substantial dimming of the SN light. Ordinary dust absorbs predominantly in the blue, leading to a reddening of the SN colors. The amount of reddening can be measured, and from it, the amount of extinction can be determined, provided the extinction law (extinction as a function of wavelength) is known. The usual extinction law [16] reads:

$$m_j \to m_j + A_V \left(a(\lambda_j) + \frac{b(\lambda_j)}{R_V} \right) = m_j + E(B-V) \left(R_V a(\lambda_j) + b(\lambda_j) \right) , \quad (3.3)$$

where $E(B-V)$ is the excess $B-V$ color over the expected one, $R_V \approx 3.1$ in near-by galaxies is sometimes called the extinction law, $A_V = R_V E(B-V)$ is the increase in magnitude in the V-band due to dust, $a(\lambda)$ and $b(\lambda)$ are known functions, with $a(\lambda_V) = 1$, $b(\lambda_V) = 0$, and all wavelengths are in the SN rest frame. In order to correct m_j we need to know $E(B-V)$ and R_V. The former can be determined from photometry in at least two bands. The latter is more complicated. Although it can in principle be measured directly from three-band photometry, in practice, the lever-arm is limited. Furthermore, current surveys do not have precision photometry in three bands for all their SNe. Several alternative approaches have been used in the literature. Riess *et al.* [17] assume $R_V = 3.1$ everywhere; Astier *et al.* [18] instead determine one single effective R_V for all their distant SNe, finding a much lower value $R_V = 0.57 \pm 0.15$. However, this parameter effectively includes any other effect that might correlate SN color and magnitude. The proposed SNAP satellite mission [19] with its nine filters will determine R_V for each SN independently, since it will have precision optical and near-infrared photometry for all their SNe in at least three and up to nine bands. Clearly, given the uncertainties on the value of R_V in distant galaxies, this looks like the most conservative approach.

Alternatively, surveys can restrict themselves to SNe with low extinction, signaled either by their low measured values of $E(B-V)$ or by its location in an old elliptical galaxy where star formation has long ceased and dust

presence is minimal. Fig. 5 shows a w_0–w_a contour plane with the qualitative effect of dust correction through measurement of A_V and R_V from data (which increases the contour size significantly), and of uncorrected dust biases (which displace the contour).

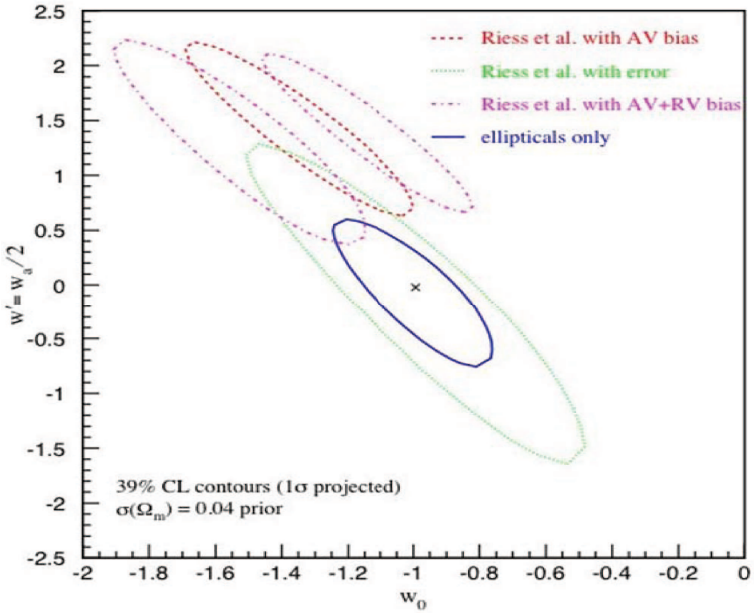

Fig. 5. Example of the increase of errors due to dust extinction correction, and of biases due to uncorrected extinction.

"Gray" dust, with an effective $R_V \to \infty$, had been postulated as an explanation for the observed dimming of SNe at large redshift. The correction method outlined above would not work for a dust that would dim equally all wavelengths. However, natural models of gray dust would lead to dimming of all SNe at all redshifts. This has been excluded by [17, 20], which have observed SNe at redshifts beyond $z = 1$ and found them to be brighter, not dimmer, than expected by models without dark energy, and in perfect agreement with the prediction of the "concordance" model: $\Omega_{\rm M} \approx 0.25$, $\Omega_\Lambda \approx 0.75$.

Flux calibration (the determination of the zero points $\phi_{0,j}$ for each filter j) can be another important source of systematic errors. While the overall normalization is irrelevant (since it can be absorbed in the unknown parameter $\mathcal{M}$ in Eq. (3.2)), the relative filter-to-filter normalizations are crucial, as they influence, for instance, the determination of colors, which are needed for the dust-extinction corrections (as we saw in the previous section), K-corrections, *etc.*

The standard procedures use well-understood stars or laboratory light sources to achieve values of $\sigma_{\rm cal}$ around few per cent in flux. A complementary procedure has been presented in [21] which uses supernova data themselves to achieve a large degree of self-calibration. For example, Fig. 6 show that for a fiducial survey close to the SNAP mission specifications, the procedure of [21] achieves an effective factor 5 reduction in calibration error.

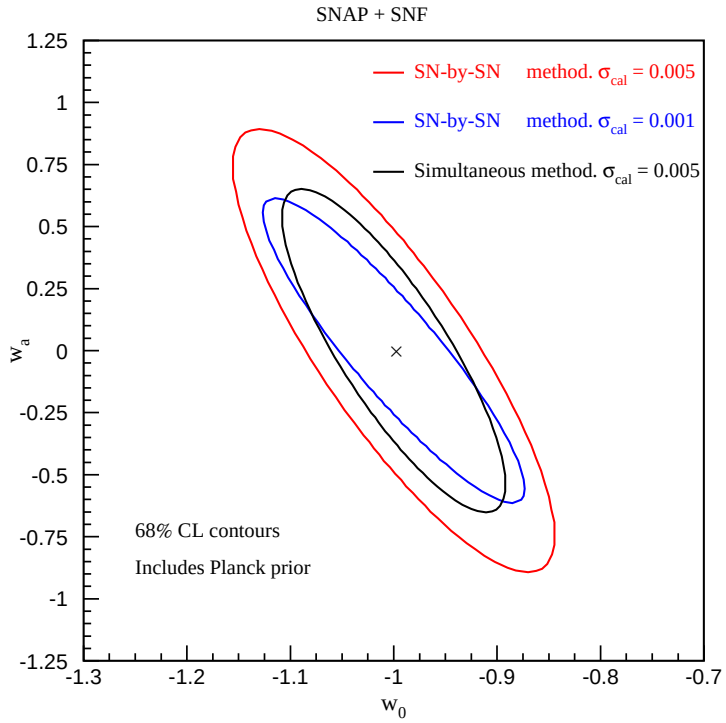

Fig. 6. Effect of self-calibration in a survey similar to the one proposed by the SNAP collaboration. Using the procedure in [21] and assuming an external calibration error of 0.005 is roughly equivalent to using the standard procedure with an external error of 0.001.

3.2. Weak lensing

The weak lensing technique is based on the statistics of the distortion ("shear") of the shape of distant galaxies produced by intervening dark matter. The effect depends on the distances between background galaxies, lenses and observer and, hence, on the geometry of the universe, but also on the foreground mass distribution, which depends on the growth of structure.

The effect is tiny and therefore huge surveys measuring shapes of close to a billion galaxies with absolute precisions of order 0.01 are needed. The main systematic worry is the very accurate knowledge of the Point Spread Function (PSF) of the system that is needed. In this regard, projects on satellites have a definitive advantage over ground-based surveys, which have to deal with changing atmospheric conditions.

Since weak lensing is a statistically very powerful dark energy probe, if it can be proven that systematic effects (particularly those related to the PDF) are under control, weak lensing might be the ultimate technique for determining the nature of dark energy.

3.3. BAO

Baryon Acoustic Oscillations are produced by acoustic waves in the photon–baryon plasma generated by primordial perturbations [22]. At recombination ($z \sim 1100$), the photons decouple from the baryons and start to free stream, whereas the pressure waves stall. As a result, baryons accumulate at a fixed distance from the original overdensity. This distance is equal to the sound horizon length at the decoupling time, $r_{\rm BAO}$. The result is a peak in the galaxy–galaxy correlation function at the corresponding scale. First detections of this excess were recently reported, at a significance of about three standard-deviations, both in spectroscopic [23–25] and photometric [26] galaxy redshift surveys. Fig. 7, taken from [23], shows the galaxy–galaxy correlation function using Luminous Red Galaxies (LRGs), with the prominent BAO peak.

The comoving BAO scale is accurately determined by CMB observations ($r_{\rm BAO} = 146.8 \pm 1.8$ Mpc for a flat ΛCDM Universe [27]), and constitutes a "standard ruler" of known physical length. The existence of this natural standard ruler, measurable at different redshifts, makes it possible to probe the expansion history of the universe, and thereby the universe geometry and dark energy properties (see, *e.g.*, [28, 29] and references therein), much like standard candles like type-Ia SNe do. This motivates the present efforts to measure BAOs (*e.g.*, [30–38]).

Broad-band photometric galaxy surveys can measure the angular scale of $r_{\rm BAO}$ in several redshift shells, thereby determining $(1+z)d_{\rm A}(z)/r_{\rm BAO}$, where $d_{\rm A}(z)$ is the angular distance to the shell at redshift z. If galaxy redshifts can be determined precisely enough, the BAO scale can also be measured along the line of sight, providing a direct measurement of the instantaneous expansion rate, the Hubble parameter (or actually of $H(z)\, r_{\rm BAO}$), at different redshifts. The direct determination of $H(z)$ distinguishes the BAO method from other methods. In addition, since systematic errors affect the radial and tangential measurements in different ways, the consistency between the measured values of $H(z)$ and $d_{\rm A}(z)$ offers a test of the results.

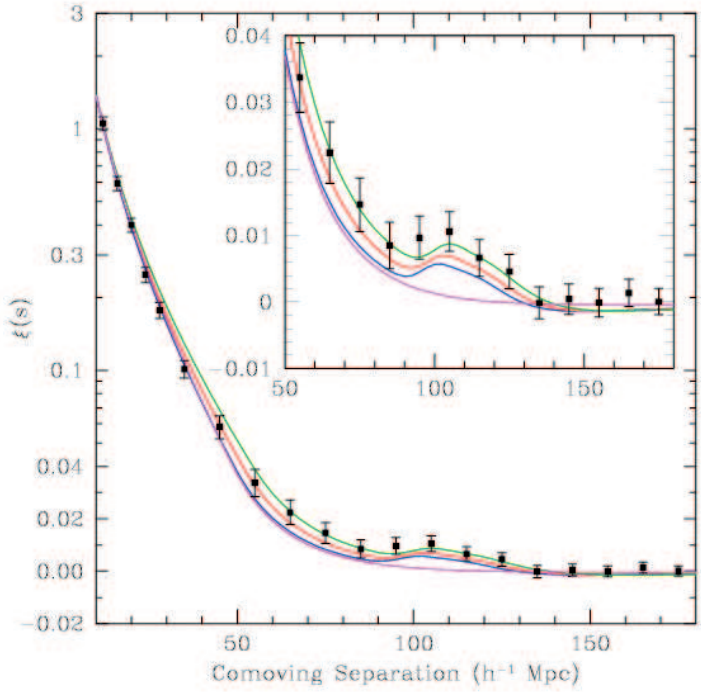

Fig. 7. The galaxy–galaxy correlation function measured using LRGs from the SDSS spectroscopic sample [23]. The BAO peak is clearly seen at about 100 Mpc/h.

As a rule of thumb, in order to get the same sensitivity to the dark-energy parameters, a galaxy redshift survey capable of exploiting the information along the line of sight needs to cover only $\sim 10\%$ of the volume covered by a comparable survey that detects the scale in the transverse direction only [39].

Large volumes have to be surveyed in order to reach the statistical accuracy needed to obtain relevant constraints on dark-energy parameters. Enough galaxies must be observed to reduce the shot noise well below the irreducible component due to sampling variance. The usefulness of the correlation along the line of sight favors spectroscopic redshift surveys that obtain very accurate redshifts, but the need for a large volume favors photometric redshifts that can reach down to fainter galaxies. Both approaches are being pursued actively around the world.

3.4. Clusters

Galaxy clusters are the largest collapsed structures in the universe. Their mass density function $dn/dV\,dM$ can be predicted and it depends on dark energy through the equations of growth of structure. The measured cluster density involves both the mass density function and the volume element, which depends on dark energy through geometry:

$$\frac{dn}{dz d\Omega} = \frac{dV}{dz d\Omega} \int\limits_{M_{\rm lim}}^{\infty} dM \frac{dn}{dV\,dM}$$

with

$$\frac{dV}{dz d\Omega} = \frac{r^2(z)}{H(z)}$$

the volume element. Learning about cosmology from clusters requires a clean way to select them, and estimate their redshift, and most importantly, finding observables that relate to the cluster mass. These can be measurements of the hot gas in the cluster (Sunyaev–Zel'dovich effect in the CMB, X-ray emission), of the galaxies and their luminosity (optical astronomy) or, directly, of the dark matter mass (weak lensing). Being able to perform mass cross-calibration using several of these techniques is an important asset that the DES survey (described in Section 5.1) in conjunction with the South Pole Telescope (SPT) posseses.

Cluster counting remains the most uncertain method for determining dark energy properties, with both a great potential and big challenges.

4. Current status

The current understanding of dark energy can be summarized by Fig. 8, taken from [40]. While if one assumes a constant equation of state w, its value is constrained to be within about 10% of -1, the value for a cosmological constant, as soon as the assumption of constant w is dropped, the constrain weakens to the point of being useless (right plot in Fig. 8). The next generation of surveys will try to learn about the possible dependence of w with cosmic time.

5. Future surveys

5.1. DES

The Dark Energy Survey (DES) is an international project, led by Fermilab (USA) whose main goal is to survey 5000 sq. deg. of the southern galactic sky, measuring positions on the sky, shapes and redshifts of about

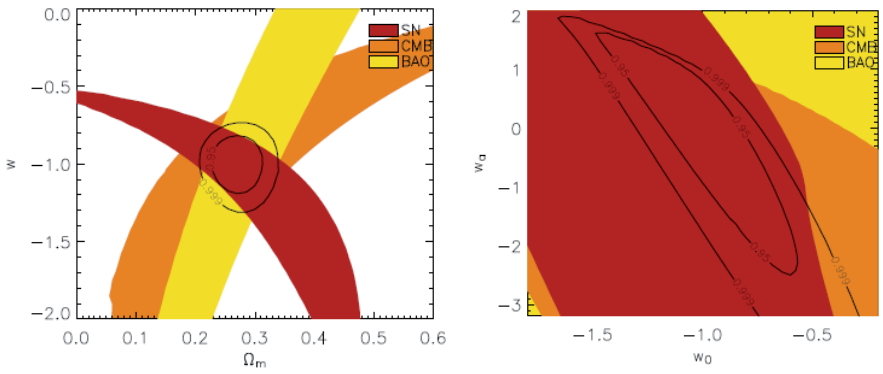

Fig. 8. Left: Current world 68% confidence-level contours in the Ω_m–w plane, assuming a flat universe and a constant equation of state w. Right: 68% confidence-level contours in the w_0–w_a plane for the world combined data from SNe, BAO and CMB. A flat universe has been assumed. Figure taken from [40].

300 million galaxies and (in conjunction with the South Pole Telescope) 15000 galaxy clusters. Furthermore, another 10 sq. deg. of the sky will be repeatedly monitored with the goal of measuring magnitudes and redshifts of over 1000 distant type-Ia SNe. These measurements will allow detailed studies of the properties dark energy using the four probes advocated in [3].

To perform the survey, the DES Collaboration is building a large wide-field CCD camera (DECam) that will give images covering 3 sq. deg. on the sky. The camera, shown in Fig. 9, will be mounted at the prime focus of the 4-meter Blanco Telescope, located in Cerro Tololo in Chile. In return, DES is granted 30% of all the observation time for 5 years (2011–2015).

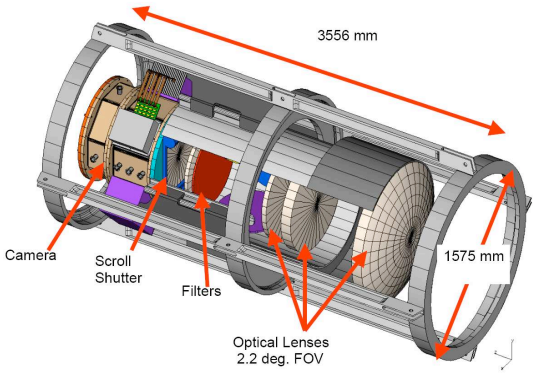

Fig. 9. A view of DECam, the camera being built by DES.

Being able to measure redshifts accurately is central to the whole DES science program. This is area of much active research within the collaboration, which will also benefit from the VHS survey in ESO's VISTA telescope, that will cover the same area of the sky in the near infrared. Combining the four techniques DES will be able to determine the dark energy equation if state parameters very precisely, as shown in Fig. 10.

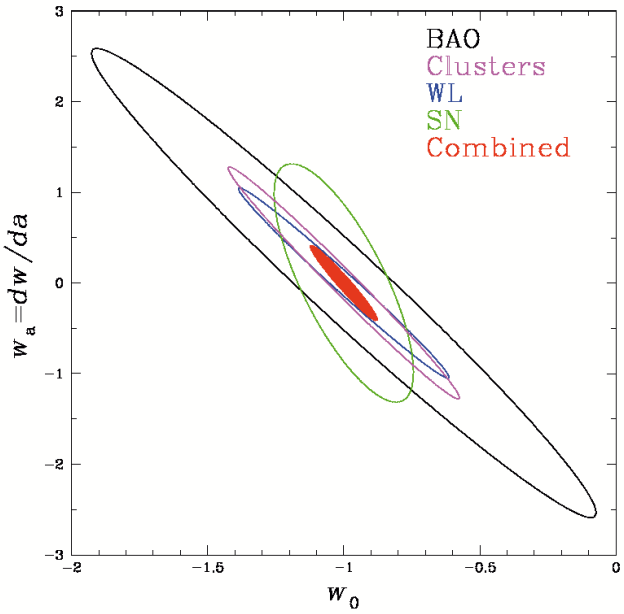

Fig. 10. 68% confidence-level contours in the w_0–w_a plane for the four techniques DES will use and their combination.

5.2. SNAP

Of the proposed supernova surveys in the next decade, the SuperNova Acceleration Probe (SNAP) satellite mission is probably the most ambitious. In essence, it consists of a 2 m-class wide-field (0.7 deg^2) imager with state-of-the-art optical and near-infrared camera and an integral-field-unit spectrograph. The dual aim is to collect about 2000 type-Ia SNe up to redshift $z = 1.7$, and to study weak gravitational lensing from space. If approved, it could fly from about 2013–2015 on.

Since a space mission is always much more expensive than a ground-based survey, the first question that comes to mind is "why space"? Fig. 11 demonstrates that for a SNAP-like mission, and keeping the time of the

mission constant, there is a clear advantage in sensitivity to w_a by going to larger redshifts, $z \geq 1.5$. Furthermore, the window to the deceleration era $z > 1$ can help in eliminating systematic errors (see, for instance, the gray dust discussion in Section 3.1.2). However, for $z > 1$–1.2, the rest-frame B-band gets redshifted into the observer near infra-red region ($\lambda > 1.2\mu$m). At these wavelengths, atmospheric background makes it all but impossible to perform accurate measurements from the ground, hence the need for a space-based mission.

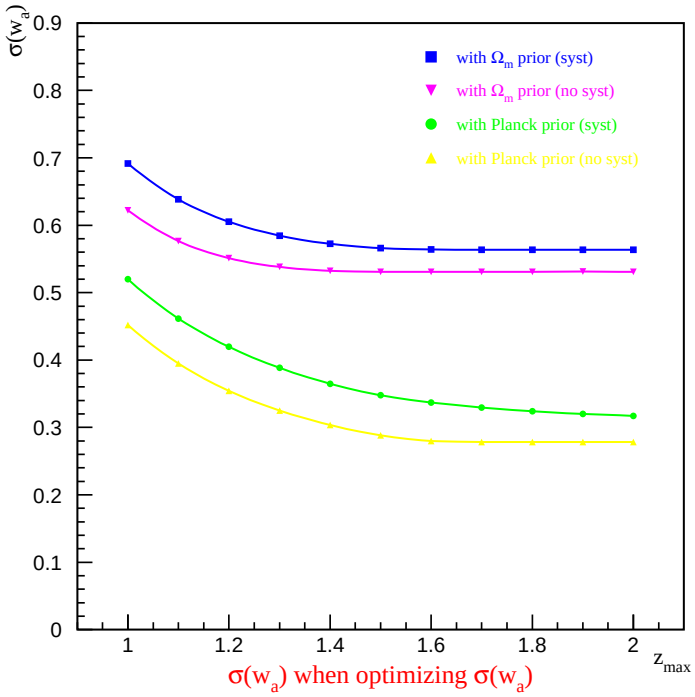

Fig. 11. Uncertainty on the w_a parameter as a function of maximum redshift $z_{\max}$ for a SNAP-like mission with fixed total time. The different lines correspond to different assumptions about priors and systematic errors.

The SNAP optical imaging system incorporates nine redshifted wide-band filters covering from the U-band to about 1.7 microns. The detectors are LBNL-developed thick, back-illuminated CCDs with quantum efficiency above 50% up to one micron, and HgCdTe detectors covering the near-infrared region. The nine filters ensure that at least there colors are available for all SNe in their restframe U to R wavelength range. This information can be used to determine the reddening law R_V individually for each supernova, eliminating a potentially damaging systematic uncertainty.

The large number of SNe in each redshift bin will also allow to tackle the issue of "evolution" of SNe properties with redshift. This has been often mentioned as a potentially dangerous source of systematic errors. By taking multi-color light-curves and multi-epoch spectra for all the supernovae, SNAP will be able to classify them according to their observational differences. Then, cosmology can be extracted by performing cosmology fits within each sub-type, each including both low- and high-redshift SNe ("like-to-like" comparison). In practice, this is done by allowing a different value of the nuisance parameter $\mathcal{M}$ for each sub-type. It has been shown in [14] that the statistical degradation due to the extra free parameters in the fit is only of a few per cent.

Fig. 12 shows the expected SNAP precision in the w_0–w_a plane. SNAP with SNe and weak lensing can, by itself, determine w_0 to about 5%, and $w' \approx w_a/2$ to about 10%.

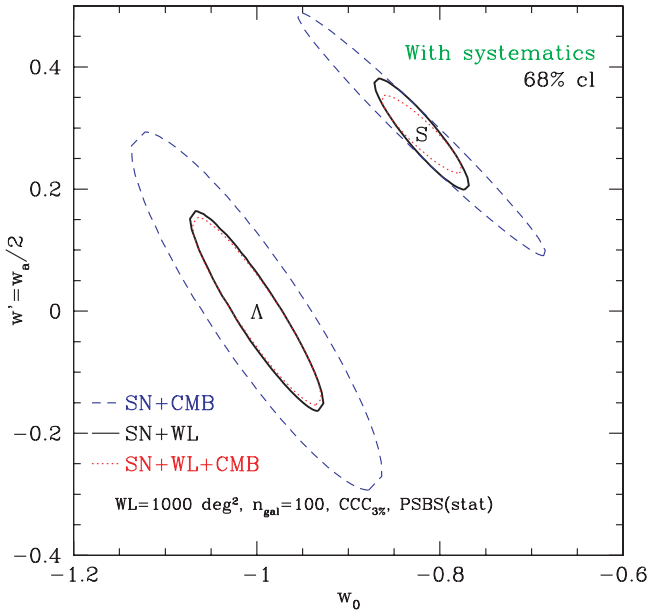

Fig. 12. Expected reach of the SNAP satellite mission. The "Λ" contours correspond to assuming a ΛCDM fiducial universe, while the "S" contours correspond to a Supergravity-inspired model. The "Λ" universe tends to lead to the most conservative contours. Note in both cases the big improvement after adding weak lensing.

5.3. PAU

It has usually been assumed in the literature that photometric redshifts are not precise enough to measure "line-of-sight" BAO [28, 39]. The intrinsic comoving width of the peak in the mass correlation function is about 15 Mpc/h, due mostly to Silk damping [41]. This sets a requirement for the redshift error of order $\sigma(z) = 0.003(1+z)$, corresponding to 15 Mpc/h along the line of sight at $z = 0.5$. A much better precision will result in oversampling of the peak without a substantial improvement on its detection, while worse precision will, of course, result in the effective loss of the information in the radial modes [28].

The PAU (Physics of the Accelerating Universe) survey [38] aims at a redshift accuracy of $\sigma(z) = 0.003(1 + z)$ for luminous red galaxies using photometry with a system of 40 filters of $\sim$ 100 Å, continuously covering the spectral range from $\sim$ 4000 to $\sim$ 8000 Å, plus two additional broad-band filters similar to the u and z-bands. PAU will measure positions and redshifts for over 14 million luminous red galaxies over 8000 deg^2 in the sky, in the range $0.1 < z < 0.9$ (comprising a volume of 9 (Gpc/h)^3). The PAU survey can be carried out in a four year observing program at a dedicated telescope with an effective *etendue* $\sim$ 20 m^{2}deg^2.

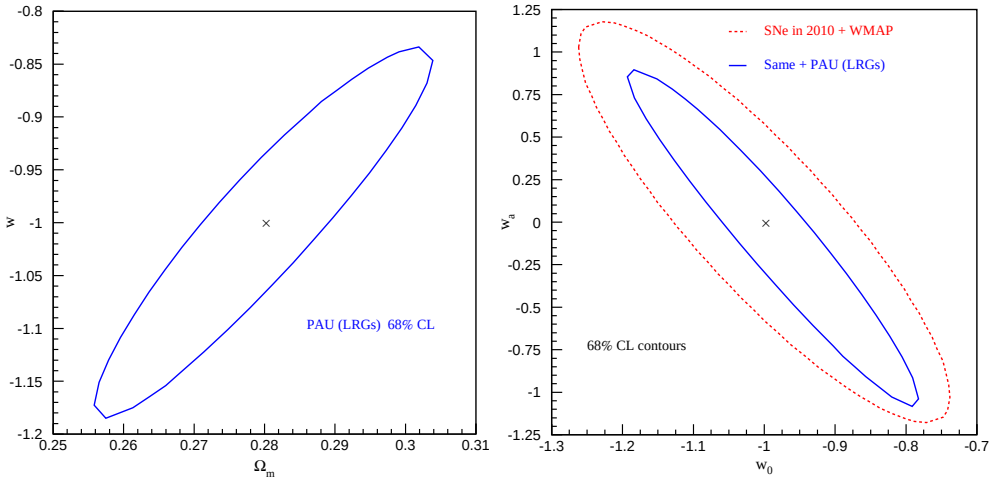

Fig. 13. Left: 68% confidence-level contours in the Ω_m–w plane, using only PAU LRG data, assuming a flat universe and a constant equation of state w. Right: 68% confidence-level contours in the w_0–w_a plane for the world combined data from SNe and WMAP in about 2010, and after adding PAU LRG data to that data set. The area of the contour decreases by about a factor three. A flat universe has been assumed.

At the end of the survey, both $H(z)r_{\rm BAO}$ and $(1+z)d_{\rm A}(z)/r_{\rm BAO}$ will have been measured in 16 bins in redshift between $z = 0.1$ and $z = 0.9$ with a relative precision that improves monotonically with increasing redshift, flattening out at about 5% for $H(z)$ and 2% for $d_{\rm A}(z)$. The left panel of Fig. 13 shows the 68% confidence level (CL) contour in the Ω_m–w plane that can be achieved using only PAU LRG data. The corresponding one-sigma errors are $\sigma(\Omega_m, w) = (0.016, 0.115)$. A flat universe and constant equation of state has been assumed. In the right panel of Fig. 13, 68% CL contours are shown in the w_0–w_a plane, assuming a flat universe. The outermost contour approximates the expected world combined precision from SNe and WMAP when PAU will start taking data, while the inner contour adds the PAU LRG data to the previous data set. The area is reduced by about a factor three. The one-sigma errors are $\sigma(w_0, w_a) = (0.14, 0.67)$.

6. Summary

In 1998, the discovery of the accelerated expansion of the universe changed completely our understanding of the universe and its components. Ten years on, the quest to understand what causes the acceleration continues. New observational projects from the ground will provide very useful information, in particular starting to probe the time dependence of the equation of state parameter w, starting around 2010. Furthermore, if approved, one or two satellite projects will measure dark energy properties with exquisite precision from about 2015 on. Along the way, the most ambitious photometric and spectroscopic surveys ever will be used for many other cosmological and astrophysical studies.

It is a pleasure to thank the organizers of the conference and in particular Antonio Bueno and Francisco del Águila for their kind invitation, for running the conference so smoothly, and for making our stay in Baeza so enjoyable.

REFERENCES

[1] S. Perlmutter *et al.*, *Astrophys. J.* **517**, 565 (1999) [arXiv:astro-ph/9812133].

[2] A.G. Riess *et al.*, *Astron. J.* **116**, 1009 (1998) [arXiv:astro-ph/9805201].

[3] A. Albrecht *et al.*, arXiv:astro-ph/0609591v1.

[4] D.A. Howell *et al.*, *Nature* **443**, 308 (2006) [arXiv:astro-ph/0609616].

[5] M.M. Phillips, *Astrophys. J.* **413**, L105 (1993).

[6] S. Perlmutter *et al.*, *Astrophys. J.* **483**, 565 (1997) [arXiv:astro-ph/9608192].

[7] M. Hamuy, M.M. Phillips, J. Maza, N.B. Suntzeff, R.A. Schommer, R. Aviles, *Astron. J.* **109**, 1669 (1995).

[8] A.G. Riess, W.H. Press, R.P. Kirshner, *Astrophys. J.* **473**, 88 (1996) [arXiv:astro-ph/9604143].

[9] J.L. Tonry *et al.*, *Astrophys. J.* **594**, 1 (2003) [arXiv:astro-ph/0305008].

[10] M. Chevallier, D. Polarski, *Int. J. Mod. Phys.* **D10**, 213 (2001) [arXiv:gr-qc/0009008].

[11] E.V. Linder, *Phys. Rev. Lett.* **90**, 091301 (2003) [arXiv:astro-ph/0208512].

[12] http://snfactory.lbl.gov

[13] M. Sako *et al.*, In the Proceedings of 22nd Texas Symposium on Relativistic Astrophysics at Stanford University, Stanford, California, Dec. 13–17, 2004, pp. 1424 [arXiv:astro-ph/0504455].

[14] A.G. Kim, E.V. Linder, R. Miquel, N. Mostek, *Mon. Not. R. Astron. Soc.* **347**, 909 (2004) [arXiv:astro-ph/0304509].

[15] D.J. Schlegel, D.P. Finkbeiner, M. Davis, *Astrophys. J.* **500**, 525 (1998) [arXiv:astro-ph/9710327].

[16] J.A. Cardelli, G.C. Clayton, J.S. Mathis, *Astrophys. J.* **345**, 245 (1989).

[17] A.G. Riess *et al.*, *Astrophys. J.* **607**, 665 (2004) [arXiv:astro-ph/0402512].

[18] P. Astier *et al.*, *Astron. Astrophys.* **447**, 31 (2006) [arXiv:astro-ph/0510447].

[19] http://snap.lbl.gov

[20] R.A. Knop *et al.*, *Astrophys. J.* **598**, 102 (2003) [arXiv:astro-ph/0309368].

[21] A.G. Kim, R. Miquel, *Astropart. Phys.* **24**, 451 (2006) [arXiv:astro-ph/0508252].

[22] D.J. Eisenstein, W. Hu, *Astrophys. J.* **496**, 605 (1998).

[23] D.J. Eisenstein *et al.*, *Astrophys. J.* **633**, 560 (2005) [arXiv:astro-ph/0501171].

[24] W.J. Percival, S. Cole, D.J. Eisenstein, R.C. Nichol, J.A. Peacock, A.C. Pope, A.S. Szalay, *Mon. Not. R. Astron. Soc.* **381**, 1053 (2007).

[25] G. Hütsi, *Astron. Astrophys.* **449**, 891 (2006).

[26] N. Padmanabhan *et al.*, *Mon. Not. R. Astron. Soc.* **378**, 852 (2007).

[27] G. Hinshaw, arXiv:0803.0732v1 [astro-ph].

[28] J.J. Seo, D.J. Eisenstein, *Astrophys. J.* **598**, 720 (2003).

[29] C. Blake, K. Glazebrook, *Astrophys. J.* **594**, 665 (2003).

[30] http://www7.nationalacademies.org/ssb/BE_Nov_2006_bennett.pdf

[31] http://www.darkenergysurvey.org

[32] http://www.as.utexas.edu/hetdex

[33] http://pan-starrs.ifa.hawaii.edu/public/

[34] http://sci.esa.int/science-e/www/object/index.cfm?fobjectid=42266

[35] B. Basett *et al.*, arXiv:astro-ph/0510272.

[36] http://astronomy.swin.edu.au/ karl/Karl-Home/Home.html
[37] http://www.sdss.org/news/releases/20080110.sdss3.html
[38] N. Benítez *et al.*, arXiv:0807.0535v1 [astro-ph].
[39] C. Blake, S. Bridle, *Mon. Not. R. Astron. Soc.* **363**, 1329 (2005).
[40] T.M. Davis *et al.*, *Astrophys. J.* **666**, 716 (2007) [arXiv:astro-ph/0701510].
[41] J. Silk, *Astrophys. J.* **151**, 459 (1968).